

# Transport Characteristics of Neutralization Dialysis and Desalination of Tap Water

Manabu Igawa,\* Kentaro Mikami, and Hiroshi Okochi

Faculty of Engineering, Kanagawa University, 3-27-1 Rokkakubashi, Kanagawa-ku, Yokohama 221-8686

(Received August 13, 2002)

In neutralization dialysis, the salt solution is desalinated continuously. The cations in desalination compartment are exchanged with protons in the acid compartment across a cation-exchange membrane and the anions are exchanged with hydroxide ions in the base compartment across an anion-exchange membrane. A simple index ( $C/J$ ), where  $C$  is the source phase concentration ( $\text{mol cm}^{-3}$ ) and  $J$  is the flux ( $\text{mol cm}^{-2} \text{min}^{-1}$ ), was proposed for the estimation of the desalination properties in neutralization dialysis. The index was based on the concepts of the ion-exchange reaction rate at the membrane interface and was related to the permeation constant in the source-phase boundary layer at the membrane interface,  $P_a$  ( $\text{cm min}^{-1}$ ), as  $C/J = 1/(k_1 \cdot C_{\text{ex}}) + 1/P_a$ , where  $k_1$  is the rate constant of ion-exchange reaction ( $\text{mol}^{-1} \text{cm}^4 \text{min}^{-1}$ ) and  $C_{\text{ex}}$  is the ion exchange capacity of the membrane ( $\text{mol cm}^{-3}$ ). The desalination efficiency increased with the decrease of the desalination compartment thickness and the decrease of the linear velocity, which can be estimated well by using the index. Tap water was desalinated by neutralization dialysis and pure water was obtained at the outlet of the desalination cell.

Neutralization dialysis is a continuous desalination method first reported in 1986,<sup>1,2</sup> which uses ion-exchange membranes and is based on Donnan Dialysis.<sup>3</sup> The desalination scheme is shown in Fig. 1. Salt solution, acid solution, and base solution flow in compartments D, A, and B. The cations in compartment D are exchanged with protons in compartment A across a cation-exchange membrane and the anions are exchanged with hydroxide ions in compartment B across an anion-exchange membrane. Therefore, the salt solution in compartment D is desalinated continuously. There have been some reports on the permeation properties of the method.<sup>4–9</sup> This method is useful

for the separation of non-electrolytes or organic solutes from ions.<sup>1</sup> It is also efficient to remove weak acids and bases such as silicate ions,<sup>7</sup> and the potential of this method to be used in the food industry has been reported.<sup>10,11</sup> This method can be also used in the water purification.<sup>7</sup> The feed solution was circulated in our previous works,<sup>1,2,7</sup> but the purified water is better obtained just after the outlet of the cell without circulation for desalination.

In this paper, we tried the desalination experiment without circulation of the feed solution. We will propose at first a simple index ( $C/J$ ), where  $C$  is the source phase concentration ( $\text{mol cm}^{-3}$ ) and  $J$  is the flux ( $\text{mol cm}^{-2} \text{min}^{-1}$ ), to estimate the desalination properties in neutralization dialysis. In the derivation of the index, we do not depend on the concepts of the conventional quasi-equilibrium but on the ion-exchange reaction rate at the membrane interface<sup>12</sup> to interpret the transport phenomena accurately. Next, we will discuss the desalination properties of the neutralization dialysis by using this index. Finally, we will report the result of the tap water desalination by neutralization dialysis.

## Experimental

**Apparatus.** Neutralization dialysis was carried out in the cell shown in Fig. 2. The feed solution, the acid solution, and the base solution were circulated in the previous research,<sup>7</sup> but in this paper, the feed solution was not circulated, although the acid and the base solutions were circulated at a rate of  $100 \text{ cm}^3 \text{min}^{-1}$ . The solutions were pumped from the reservoirs with tubing pumps and the feed solution was collected for analysis just after the outlet of the desalination cell. The compartments in the cell were labeled as follows: compartment D for the feed solution, compartment A for the acid solution, and compartment B for the base solution. Each membrane area was  $30 \text{ cm}^2$  ( $2 \text{ cm} \times 15 \text{ cm}$ ), the thickness of

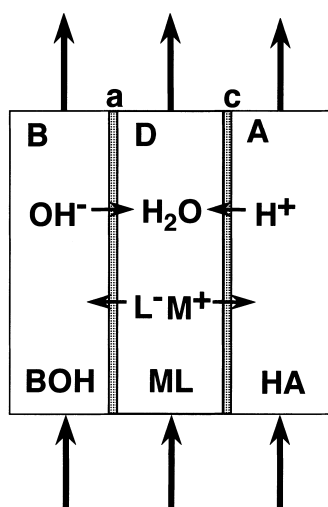


Fig. 1. Schematic ion transport. a, anion-exchange membrane; c, cation-exchange membrane; A, acid solution compartment; D, desalination compartment; B, base solution compartment; ML, salt, HA, acid; BOH, base.

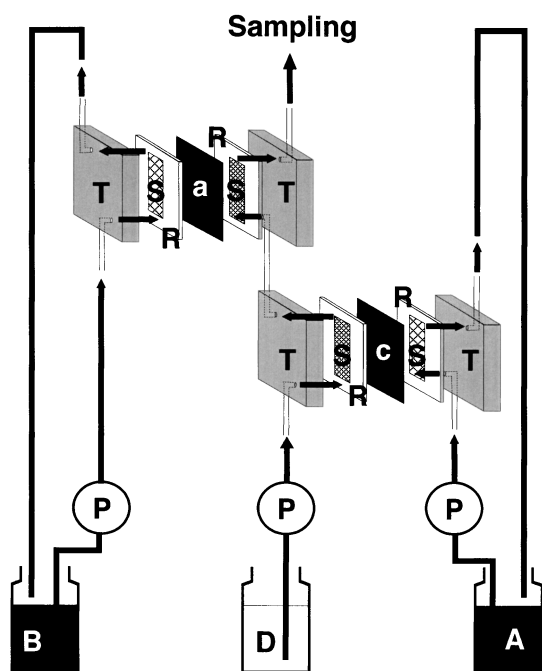


Fig. 2. Neutralization dialysis cell. a, anion-exchange membrane; c, cation-exchange membrane; R, Viton rubber sheet; S, spacer; T, Teflon plate; P, tubing pump

each compartment was 1.0 mm, and a net type spacer 1.0 mm thick was placed in each compartment, unless otherwise stated. The apparatus used in this study are two two-compartment cells; they are shown in Fig. 2. A cation- and an anion-exchange membrane, Selemion CMV and AMV (Asahi Glass Co. Ltd.), were used in this study. In the desalination of tap water, tap water in our laboratory was pretreated with ultrafiltration (Millipore Mini-Plate-3, molecular cut-off 3000). Purified nitrogen gas was bubbled into the water in its reservoir to purge the dissolved carbon dioxide. Then, the water was desalinated by neutralization dialysis with three sets of two two-compartment cells; the total membrane area of each cation- and anion-exchange membrane was 90 cm<sup>2</sup>.

**Analysis.** A resistivity meter (Toa Denpa Ind. Co. Ltd.) was placed in the line just after the outlet of the desalination compartment D to measure the specific conductivity (SC) of the desalinated water continuously. The desalinated water collected just after the outlet of the desalination cell were analyzed for major cations, anions, dissolved silica, and dissolved organic carbon (DOC). These components were analyzed by the following apparatus: Na<sup>+</sup> and K<sup>+</sup>, an atomic absorption spectrophotometer (Shimadzu AA-6700F); Cl<sup>-</sup>, an ion chromatograph (Dionex-100); Ca<sup>2+</sup>, Mg<sup>2+</sup>, and dissolved silica, an inductively-coupled plasma atomic emission spectrophotometer (Seiko SPS1500); DOC, a total organic carbon analyzer (Shimadzu TOC-5000).

### Results and Discussion

Diffusion flux is very important in the evaluation of the desalination characteristics in neutralization dialysis and it can be obtained by considering the diffusion across not only the membrane phase but also the boundary layers adjacent to the membrane in the source and receiving phases. The cation flux and the proton flux have the reverse direction and the same value in the cation-exchange membrane, as shown in Fig. 3, where the

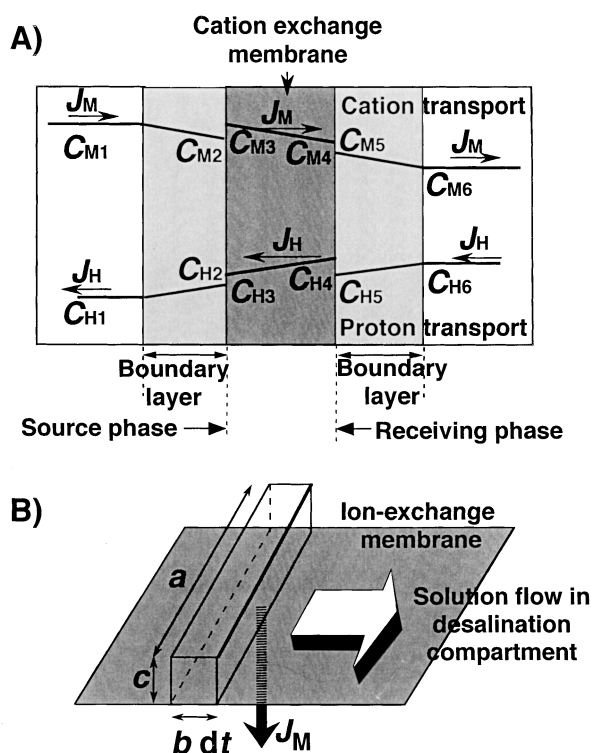


Fig. 3. Counter transport of cation and hydrogen ion across a cation-exchange membrane (A) and salt flux in desalination compartment (B). a, compartment width; c, compartment thickness; b, linear velocity of the solution flow; dt, differential time in solution transfer.

meanings of the symbols are also shown. There are analogous phenomena for some anions and hydroxide ion in the anion-exchange membrane. The flux across the cation-exchange membrane is equal to the flux in the boundary layer, and it can be written as follows.

$$J = P_a (C_{M1} - C_{M2}) = P_a (C_{H1} - C_{H2}) \quad (1)$$

where  $P_a$  is a permeation constant in the boundary layer (cm min<sup>-1</sup>). An ion-exchange reaction occurs at the surface of the membrane and it is correlated to the flux as follows:

$$J = k_1 \cdot C_{M2} \cdot C_{H3} - k_{-1} \cdot C_{M3} \cdot C_{H2} \quad (2)$$

where  $k_1$  and  $k_{-1}$  are the rate constants (mol<sup>-1</sup> cm<sup>4</sup> min<sup>-1</sup>) of ion-exchange reaction per unit membrane area in the metal ion uptake and the splitting at the surface of the ion-exchange membrane, respectively. The surface concentrations of  $C_{M2}$  and  $C_{H2}$  are eliminated by substituting Eq. 1 to Eq. 2, and Eq. 3 is obtained.

$$J = (k_1 \cdot C_{M1} \cdot C_{H3} - k_{-1} \cdot C_{M3} \cdot C_{H1}) / \{1 + (k_1 \cdot C_{H3} - k_{-1} \cdot C_{M3}) / P_a\} \quad (3)$$

In most of the cases, except high concentration of the solution in desalination compartment, the following two conditions,  $C_{H1} \ll C_{M1}$  and  $C_{M3} \ll C_{H3}$ , can be applied. Then, Eq. 3 can be simplified as Eq. 4:

$$J = k_1 \cdot C_{M1} \cdot C_{H3} / (1 + k_1 \cdot C_{H3} / P_a) \quad (4)$$

Furthermore,  $C_{H3}$  is approximately equal to the ion exchange capacity of the membrane,  $C_{ex}$  (mol cm<sup>-3</sup>), and Eq. 4 can be modified as follows:

$$C/J = 1/(k_1 \cdot C_{ex}) + 1/P_a \quad (5)$$

where the terms in right-hand side are constant, although  $P_a$  depends on the linear velocity of the solution in the desalination compartment, and  $C$  is used instead of  $C_{M1}$  to simplify the discussion. For anions, the analogous equations can be obtained at the interface of the anion-exchange membrane.

To compare the experimental values with the theoretical values obtained by Eq. 5, the values of  $C/J$  should be obtained. The values,  $C$  and  $J$ , change with the solution flow from the inlet to the outlet of the desalination compartment, but they can be obtained as follows. For the solution with the volume of  $a \cdot c \cdot b \cdot dt$  in the desalination compartment, the salt flux across the membrane can be defined as follows.

$$J = -dC \cdot a \cdot c \cdot b \cdot dt / (dt \cdot a \cdot b \cdot dt) = -dC \cdot c / dt = C/A \quad (6)$$

where  $a$  is the compartment width (cm),  $c$  is the compartment thickness (cm),  $b$  is the linear velocity of the solution (cm min<sup>-1</sup>), and  $dt$  is the differential time (min) of the solution in the desalination compartment, which are shown in Fig. 3B. The value of  $A$  in Eq. 6 is the constant, which is equal to the right-hand side of Eq. 5. By integrating Eq. 6 ( $-dC \cdot c / dt = C/A$ ) from  $t = 0$  to  $t = t_{cell}$ , which is the residence time for the solution in the cell, Eq. 7 is obtained:

$$\ln(C_{in}/C_{out}) = t_{cell}/(A \cdot c) \quad (7)$$

In the residence time,  $t_{cell}$ , the concentration of  $C$  changes from the inlet concentration,  $C_{in}$ , to the outlet concentration,  $C_{out}$ . The concentrations of  $C_{out}$  and  $C_{in}$  were obtained by the analysis of the solution concentrations just after the outlet of the cell and in the reservoir of the compartment D, and  $t_{cell}$  was calculated from the pumping rate and the free space in the desalination cell corrected by the occupied volume of the spacer in the cell. Therefore,  $A$ , that is  $C/J$ , can be obtained by Eq. 7.

Figure 4 shows the relationship between  $C/J$  and the salt concentration in the desalination compartment. When the concentration is lower than 10 mmol dm<sup>-3</sup>, the value is nearly constant. When the concentration becomes higher,  $C_{M3}$  can not be neglected compared to  $C_{H3}$  and Eq. 5 fails. Figure 4 also shows the flux approaching a constant value with the increase of the feed concentration, which is explained as follows. The flux in the membrane phase is described as follows with the use of the permeation constant,  $P_m$  (cm min<sup>-1</sup>), in the membrane phase.

$$J = P_m (C_{M3} - C_{M4}) \quad (8)$$

When the feed concentration becomes high and the ion-exchange reaction occurs effectively at the interface between the membrane and the receiving phase,  $C_{M3}$  approaches to the ion-exchange capacity,  $C_{ex}$ ,  $C_{M3} \gg C_{M4}$ , and the flux shown in

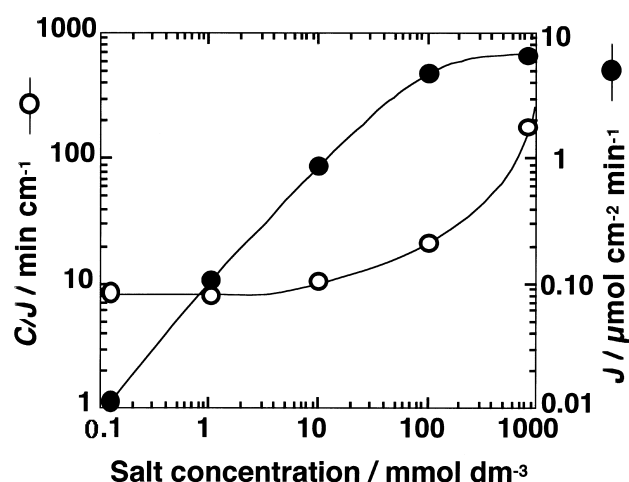


Fig. 4. Effect of salt concentration on  $C/J$ . Salt solution in desalination compartment, 0.1–1000 mmol dm<sup>-3</sup> KCl; flow rate, 3.0 cm<sup>3</sup> min<sup>-1</sup>; compartment thickness, 0.050 cm; linear velocity, 45.3 cm min<sup>-1</sup>; membrane area, 30 cm<sup>2</sup>; acid solution, 100 mmol dm<sup>-3</sup> HCl 1000 cm<sup>3</sup>; base solution, 100 mmol dm<sup>-3</sup> NaOH 1000 cm<sup>3</sup>.

Eq. 8 becomes a constant value,  $P_m \cdot C_{ex}$ , as shown in Fig. 4.

It is reported that the permeation constant is proportional to some power (from the 0.5 power to the 0.8 power) of the linear velocity at the vicinity of the boundary layer.<sup>13</sup> Then, the value,  $C/J$ , was obtained in many experimental conditions and the correlation coefficients between  $C/J$  and the reciprocal of  $x$  power of the linear velocity, where  $x$  was varied from 0.5 to 0.8, were compared to each other. The correlation coefficient was the highest (0.974), when  $x$  was 0.60. Figure 5 shows the results; the  $C/J$  value increased linearly with the reciprocal of the 0.60 power of the linear velocity as estimated by Eq. 5. The contribution of the second term in Eq. 5 to the  $C/J$  value is much larger than that of the first term. The effect of the linear velocity of the compartments A and B was also investigated,

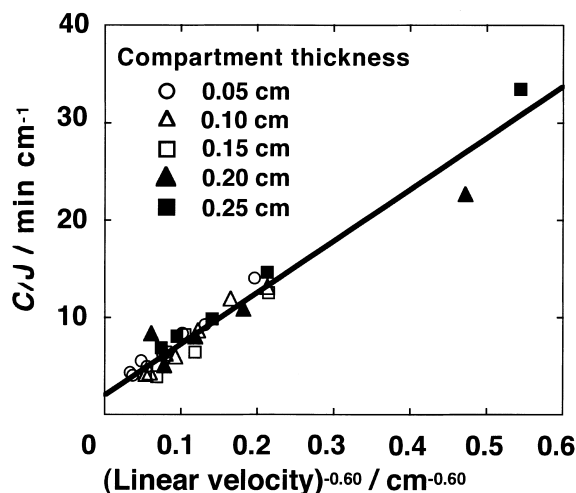


Fig. 5. Effect of linear velocity on  $C/J$ . Desalination compartment, 1.0 mmol dm<sup>-3</sup> KCl; acid solution, 100 mmol dm<sup>-3</sup> HCl 500 cm<sup>3</sup>; base solution, 100 mmol dm<sup>-3</sup> NaOH 500 cm<sup>3</sup>.

but the value,  $C/J$ , was constant and not affected by the velocity in the region of 50 to 400  $\text{cm min}^{-1}$ . Such results suggest that the rate limiting process is the boundary layer in the source phase but not the layer in the receiving phase.

By using the permeation constant, one can calculate the thickness of the boundary layer, because the permeation constant,  $P_a$ , is equal to the ratio of the diffusion coefficient to the thickness of the boundary layer. In the boundary layer,  $\text{K}^+$  and  $\text{H}^+$  are transported in the opposite direction in the experimental condition of Fig. 5, and the harmonic mean ( $1.95 \times 10^{-3} \text{ cm}^2 \text{ min}^{-1}$ ) of the diffusion coefficients of  $\text{K}^+$  and  $\text{H}^+$  is used as the diffusion coefficient<sup>14</sup> in the calculation. The thickness is calculated to be between 610  $\mu\text{m}$  to 34  $\mu\text{m}$  in the experimental condition of Fig. 5, which is reasonable, because values of the same order have been reported.<sup>9,15</sup>

The compartment thickness does not affect the value of  $C/J$  as shown in Fig. 5, but the desalination efficiency depends on the thickness. The desalination efficiency was defined as follows:

$$\text{Desalination efficiency (\%)} = (1 - C_{\text{out}}/C_{\text{in}}) \cdot 100 \quad (9)$$

Figure 6 shows the measured and the estimated efficiency vs linear velocity for the compartment thicknesses of 0.05, 0.10, and 0.25 cm. It can be estimated as follows by using Eq. 7.

$$\text{Desalination efficiency (\%)} = (1 - C_{\text{out}}/C_{\text{in}}) \cdot 100 = [1 - \exp(-t_{\text{cell}}/(c \cdot C/J))] \cdot 100 \quad (10)$$

The value of  $C/J$  is obtained from Fig. 5;  $t_{\text{cell}}$  is obtained as the ratio of the cell length, 15 cm in this experiment, to the linear velocity; the efficiency can be calculated by Eq. 10. The lines are theoretical values, and they agreed well with the measured values obtained by the analysis of  $C_{\text{out}}$  and  $C_{\text{in}}$ . The desalination efficiency increased with the decrease of the desalination compartment thickness,  $c$ , and the decrease of the value of  $C/J$ . With the increase of the linear velocity, the value of  $C/J$  decreases, as shown in Fig. 5, but the desalination efficiency decreases with the increase of the linear velocity for a constant cell length, because  $t_{\text{cell}}$  is inversely related to the velocity and the ratio of the salt flux to the pumping rate decreases with the increase of the pumping rate. By developing these equations, the desalination efficiency can be predicted from the experimental conditions. These equations are useful and can be

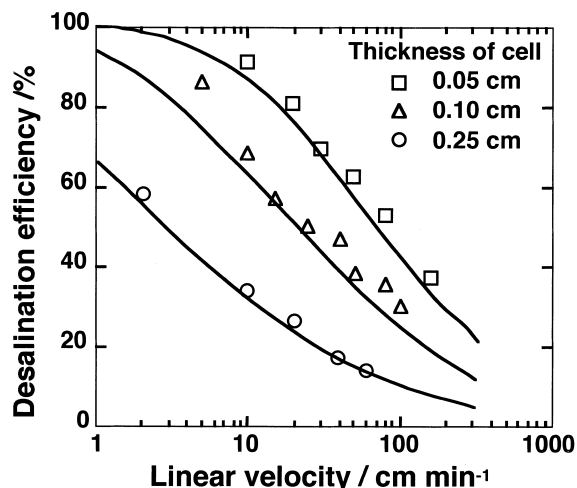


Fig. 6. Effect of linear velocity on desalination efficiency. Desalination compartment,  $1.0 \text{ mmol dm}^{-3} \text{ KCl}$ ; acid solution,  $100 \text{ mmol dm}^{-3} \text{ HCl}$   $500 \text{ cm}^3$ ; base solution,  $100 \text{ mmol dm}^{-3} \text{ NaOH}$   $500 \text{ cm}^3$ ; membrane area,  $30 \text{ cm}^2$ .

applied not only to neutralization but also to other transport phenomena, where the transport process in the source-phase boundary-layer at the interface of the ion-exchange membrane is the rate-limiting process.

Table 1 shows the result of the desalination of tap water, which was pretreated with ultrafiltration to remove polymers with large molecules. Pure water was obtained at the outlet of the desalination cell. The dissolved organic carbon was not well removed by neutralization dialysis, while multivalent metal ions were removed efficiently. For the improvement of the purity of the desalinated water, the tap water should be pretreated by reverse osmosis to remove DOC, which hardly permeates across ion-exchange membranes. As shown in Table 1, silicate ion was eliminated efficiently in this method and it is one of the advantages of neutralization dialysis, because silicate ions remaining in the treated water become an important problem for the super-pure water.

From Eq. 10, we can design the size of the neutralization dialysis membrane required to obtain desalinated water with a flow rate and a purity level desired. When we need the desalination efficiency of 99% and manufacture a cell compartment with 0.050 cm thickness, 50 cm width, and the linear velocity

Table 1. Quality of Tap Water Purified by Ultrafiltration (UF) and Neutralization Dialysis (ND)

Water	$\text{Na}^+$	$\text{K}^+$	$\text{Ca}^{2+}$	$\text{Mg}^{2+}$	$\text{Si}$	DOC	SC
	$\text{mmol dm}^{-3}$					$\text{ppmC}$	$\mu\text{S cm}^{-1}$
Tap water	0.976	0.0338	0.338	0.170	0.352	14.5	131
Pretreated with UF	0.380	0.0399	0.334	0.174	0.352	18.7	131
Purified by ND	0.0161	0.0010	0.0022	0.0007	0.0033	15.3	2.4
Desalination efficiency (%)	95.8	97.5	99.3	99.6	99.1	18.2	98.2

UF, ultrafiltration with a filter (Millipore MiniPlate-3, molecular cut-off 3000); ND, neutralization dialysis with three sets of two two-compartment cells; DOC, dissolved organic carbon; SC, specific conductivity; each membrane area,  $30 \text{ cm}^2$ ; thickness of compartment D, 0.5 mm; flow rate of desalinated water,  $1 \text{ cm}^3 \text{ min}^{-1}$ ; acid solution,  $100 \text{ mmol dm}^{-3} \text{ HCl}$   $1000 \text{ cm}^3$  in the first and the second cell and  $10 \text{ mmol dm}^{-3} \text{ HCl}$   $500 \text{ cm}^3$  in the third cell; base solution,  $100 \text{ mmol dm}^{-3} \text{ NaOH}$   $1000 \text{ cm}^3$  in the first and the second cell and  $10 \text{ mmol dm}^{-3} \text{ NaOH}$   $500 \text{ cm}^3$  in the third cell.

of  $60 \text{ cm min}^{-1}$ , that is the flow rate of  $150 \text{ cm}^3 \text{ min}^{-1}$  ( $60 \text{ cm min}^{-1} \times 0.050 \text{ cm} \times 50 \text{ cm}$ ), the value of  $C/J$  is  $6.6 \text{ min cm}^{-1}$  obtained from Fig. 5 and  $t_{\text{cell}}$  required is calculated to be 1.5 min by Eq. 7. Then, the length of the membrane required for the quality of the desalinated water is calculated to be 0.90 m ( $60 \text{ cm min}^{-1} \times 1.5 \text{ min}$ ). If the tap water is pretreated with reverse osmosis, the desalination efficiency of reverse osmosis is at least 90% and the membrane area of  $0.5 \text{ m} \times 0.9 \text{ m}$  is sufficient for the desalination for the laboratory use by neutralization dialysis. For the practical use of this method, the durability of the ion-exchange membranes, especially of the anion-exchange membrane, and the leak of protons and hydroxide ions across the membranes to the desalinated water should be improved.

We appreciate the support by High-Tech Research Project from The Ministry of Education, Culture, Sports, Science and Technology and by the funds from Kurita Water And Environment Foundation.

## References

- 1 M. Igawa, K. Echizenya, T. Hayashita, and M. Seno, *Chem. Lett.*, **1986**, 237.
- 2 M. Igawa, K. Echizenya, T. Hayashita, and M. Seno, *Bull. Chem. Soc. Jpn.*, **60**, 381 (1987).
- 3 F. G. Donnan, *Chem. Rev.*, **1**, 73 (1925).
- 4 G. A. Denisov, Preprint. ONTI PNC, Pushchino (1991).
- 5 M. Bleha and G. A. Tishchenko, *J. Membr. Sci.*, **73**, 305 (1992).
- 6 K. Sato, T. Yomemoto, and T. Tadaki, *J. Chem. Eng. Jpn.*, **26**, 68 (1993).
- 7 H. Tanabe, H. Okochi, and M. Igawa, *Ind. Eng. Chem. Res.*, **34**, 2450 (1995).
- 8 G. A. Tishchenko, G. A. Denisov, L. K. Shataeva, and M. Bleha, *Collect. Czech. Chem. Commun.*, **60**, 1888 (1995).
- 9 G. A. Denisov, G. A. Tishchenko, M. Bleha, and L. K. Shataeva, *J. Membr. Sci.*, **98**, 13 (1995).
- 10 G. Wang, H. Tanabe, and M. Igawa, *J. Membr. Sci.*, **106**, 207 (1995).
- 11 A. Zheleznoz, D. Windmoller, S. Korner, and K. W. Boddeker, *J. Membr. Sci.*, **139**, 137 (1998).
- 12 M. Igawa, E. Kobayashi, A. Itakura, K. Kikuchi, and H. Okochi, *J. Phys. Chem.*, **64**, 12447 (1994).
- 13 T. G. Kaufmann and E. F. Leonard, *AIChE J.*, **14**, 110 (1968).
- 14 E. L. Cussler, "Diffusion," Cambridge University Press, New York (1984).
- 15 S. Yoshida and S. Hayano, *J. Am. Chem. Soc.*, **108**, 3903 (1986).